

Spectroscopic analysis of Ag nanoparticles embedded in glass

Jyoti Rozra, Isha Saini, Sanjeev Aggarwal, Annu Sharma*

Department of Physics, Kurukshetra University, Kurukshetra 136 119, India

*Corresponding author. Tel: (+91) 1744-238410 Ext 2130; Fax: (+91) 1744-238277; E-mail: talk2annu@gmail.com

Received: 04 January 2013, Revised: 12 March 2013 and Accepted: 17 March 2013

ABSTRACT

Structural and optical properties of Ag-glass nanocomposite, synthesized by the combined use of vacuum deposition method and subsequent thermal annealing have been studied using UV-Visible absorption spectroscopy, Field emission scanning electron microscopy (FE-SEM) along with Energy dispersive analysis of X-rays (EDAX), Transmission electron microscopy (TEM) and Photoluminescence spectroscopy. Ag-glass nanocomposites were synthesized by depositing Ag on glass slides and the resulting samples were annealed at various temperatures from 300°C to 550°C for 1 hour. The fingerprint feature of Ag nanoparticles formation i.e. the surface plasmon resonance peak is observed around 427 nm in absorption spectra of Ag-glass samples annealed at various temperatures, this confirms the formation of Ag nanoparticles in glass. The size of Ag nanoparticles has been found to increase with increase in annealing temperature. At an annealing temperature of 400°C the size of Ag nanoparticles comes out to be 4.6 nm which increases to a value of 10.0 nm at an annealing temperature of 550°C. TEM micrograph further confirms the formation of Ag nanoparticles of size 8 ± 2 nm at an annealing temperature of 550°C. Further, analysis of UV-Visible absorption and reflection data indicates towards the increase in refractive index of Ag nanoparticles doped glasses. It has been established that with the insertion of Ag nanoparticles of size 8 ± 2 nm in glass the refractive index of the resulting nanocomposite increases to a value of 1.96. The dispersion parameters such as single-oscillator energy E_0 , and the dispersion energy E_d have been discussed in terms of the Wemple-DiDomenico single-oscillator model. Photoluminescence spectra of silver glass nanocomposite have been studied and observed spectroscopic features have been correlated with various transitions of silver ions. Such studies are vital for designing optical materials for example optical communication, photonic devices etc. Copyright © 2013 VBRI press.

Keywords: Absorption spectroscopy; Ag nanoparticles; refractive index; photoluminescence.



Jyoti Rozra received her B.Sc degree in 2005, M.Sc physics degree in 2007 and M.Phil degree in 2009 from Kurukshetra University, Kurukshetra India. She is presently studying for her PhD degree in the Department of Physics, Kurukshetra University, Kurukshetra. Her research area includes formation and characterization of metal nanoparticle based nanocomposites.



Isha Saini is pursuing her Ph.D. in Physics under supervision of Dr Annu Sharma from Department of Physics, Kurukshetra University, Kurukshetra. She is working in the area of synthesis and characterization of nanocomposites. She has presented around 12 papers in National and International conferences and has received best poster award also. She received her B.Sc degree in 2006, M.Sc physics degree in 2008 and M.Phil degree in 2010 from Kurukshetra University, Kurukshetra India.



Annu Sharma is working as an Assistant Professor in physics in the Department of Physics, Kurukshetra University, Kurukshetra. Her current research interests include synthesis and characterization of nanocomposite materials; stopping power of heavy ions and effect of ion implantation on the various properties of composite materials. She received her PhD degree in Physics in 2001 from Kurukshetra University, Kurukshetra. During 2002 to 2004, she worked as an Assistant Professor for post-doctoral research with Professor Peter Sigmund at Department of

Physics, University of Southern Denmark, Odense, Denmark. There are many research publications in the refereed international journals and in symposium and conferences to her credit.

Introduction

Composite materials containing nanoscale particles of transition metals like Ag, Au, and Cu embedded in glass as the dielectric matrix are of great interest because of their potential applications in the field of photonics owing to their unique optical characteristics originating from the strong interaction between incident light and metallic

nanoparticles [1, 2]. This interaction results in collective oscillations of electron clouds, called surface plasmon resonance (SPR), at the interface of the metallic nanoparticles and the dielectric matrix. The resonance frequency of this interaction is strongly dependent on the metal, the surrounding dielectric medium, as well as the size and shape distribution of the nanoparticles [1].

Among the metals, silver nanoparticles exhibit a sharp and distinct optical response (SPR) in the visible region of electromagnetic spectrum which is extremely important for optoelectronic applications. This property makes silver nanoparticles a proper choice for surface plasmon-based components [3, 4]. Glass is an excellent host matrix for growing small metallic particles. The metallic particles can be nucleated by heat or radiation, and grown at a high temperature, resulting in a very narrow size distribution inside the glass matrix. Such optical materials, formed by growth of silver nanoparticle in glass, have a wide variety of linear and non-linear potential applications are such as sensors [2], optical storage media [5], solar cells [6], polarizers [7] or diffraction gratings [8].

Glass embedded with silver nanoparticles can be synthesized by a variety of methods like ion exchange [9, 10], ion implantation [11], low energy ion-beam mixing [12], physical vapor deposition [13] etc. Physical vapor deposition (PVD) techniques (evaporation, sputtering [14] and other hybrid and modified PVD processes) are promising methods used for the preparation of nanocomposite using a dry process. This technique offers a great deal of promise in terms of general simplicity of operation, minimal requirements for sample preparation, ease of adaptation to automated operation and potential for scale up to production levels of material throughput. Additionally, there are no problems with residual solvents as in wet chemical synthesis processes. Of the wide array of PVD techniques available for the production of thin film materials, thermal evaporation is one of the oldest, commonly available and most inexpensive methods known.

In this paper, we demonstrate a two-step dry technique for the fabrication of scalable, homogenous metal-glass nanocomposites; glass with embedded silver nanoparticles i.e. PVD technique in high vacuum followed by thermal annealing. The effect of annealing temperature on optical and structural properties of synthesized Ag-glass nanocomposite has been investigated in detail.

Experimental

Materials

Commercially available glass slides of dimensions (75mm×25mm×1.3mm) and (composition (in wt%) 71.86% SiO₂, 13.30% Na₂O, 8.69% CaO, 4.15% MgO), supplied by (Polar Industrial Corporation, Mumbai, India) were used as substrates. Silver wire was purchased from the local market. First the substrates were washed with distilled water and further cleaned with extra-pure acetone (99.5% purity) in order to remove surface contaminants.

Synthesis of silver-glass nanocomposite

In the present work, thin films of silver of thickness 2.916 kÅ were deposited on commercially available glass substrates by thermal evaporation using a “VEQCO” high

vacuum evaporation unit EU-300 under a vacuum of the order of 10⁻⁵ torr. Thickness of silver films was measured by using a quartz crystal thickness monitor during deposition of films. Prior to the Ag film deposition onto the glass substrate, surface contaminants on substrate were removed by using distilled water and acetone. Subsequently silver wire (purity, 99.9%) was kept in a tungsten filament and was evaporated for deposition (on to glass) inside the vacuum chamber. After deposition, the source heater was turned off. The film remained under vacuum till source temperature reduced to below 100°C, to avoid the oxidation of the film. Subsequently, silver deposited glass samples were annealed at various temperatures from 300°C to 550°C in air for 1 hr. After the heat treatment these samples were rinsed with concentrated HNO₃ solution to remove excess silver film adhering on the glass surface.

Absorption spectra of Ag-glass nanocomposite samples were recorded using a Shimadzu Double Beam Double Monochromator Spectrophotometer (UV-2550), equipped with an Integrating Sphere Assembly ISR-240A in the wavelength range of 190 nm to 900 nm with a resolution of 0.5 nm. All the absorption spectra were recorded keeping air as the reference, whereas for recording diffuse reflectance spectra, BaSO₄ powder was taken as the reference material. From these spectra, optical constants such as the refractive index and dielectric constant were determined.

The size, morphology and composition of the resulting Ag-glass nanocomposite samples were studied using TEM and FE-SEM alongwith EDAX. Morphology of the Ag-glass nanocomposite samples was studied using FE-SEM Quanta 200F. Ag-glass nanocomposite sample was coated with a very thin layer of gold by sputtering technique. The coated sample was then subjected to SEM studies. In order to determine the size of the silver nanoparticles embedded in the glass matrix by direct means, TEM measurements were performed using a MORGAGNI-268D transmission electron microscope operated at accelerating voltage of 70 kV. For this study, samples were prepared in the following way: A diamond scribe was utilized to scratch the surface (a few microns below) of the glass containing silver nanoparticles. Minute powder thus obtained was carefully dropped in the methanol and kept for ultrasonification. Consequently the larger glass particles settled down and the finer ones floated on the surface of the liquid. The finest layer on the surface was collected on the carbon coated copper grid for the observation.

Photoluminescence measurements of these samples were carried out using Jobin Yvon Spectrofluorometer (Spex FluoroMax-3) where a Xe lamp was employed as the excitation source.

Results and discussion

Prior to silver deposition process, the glass samples were colorless and had no measurable absorptions in the visible region. As shown in [Fig. 1 curve (a)] no SPR peak of silver nanoparticles in glass (400–430 nm) was observed, indicating that after vacuum deposition, the silver aggregation did not occur, or the silver nanoparticles were less than 1 nm in size. After annealing at a temperature of 400°C [Fig. 1 curve (b)] a broad SPR peak characteristic of silver nanoparticles starts appearing with maxima around

427 nm [15, 9]. The width of the observed SPR peak might be due to the size distribution of silver nanoparticles. When the annealing temperature is increased to 500°C, the SPR peak becomes narrow and the absorption intensity increases [Fig. 1 curves (c)]. With the further increase in annealing temperature to 550°C [Fig. 1 curves (d)], SPR peak becomes significantly narrow and absorption intensity increases further. The observed substantial increase in absorption intensity and narrowing of the full width at half maxima (FWHM) of the absorption peak with increasing annealing temperature, indicate an increase in volume fraction and size of silver nanoparticles in the glass matrix. The symmetric shape of the SPR peak [Fig. 1 curves (c) and (d)] indicates that the Ag nanoparticles formed within the glass matrix are spherical in shape. Moreover, the color of the transparent glass samples also changes from colorless to light yellow, at an annealing temperature of 400°C, which is a characteristic of Ag-nanoparticles formation [16]. With the increase in annealing temperature the darkness of yellow color also increases.

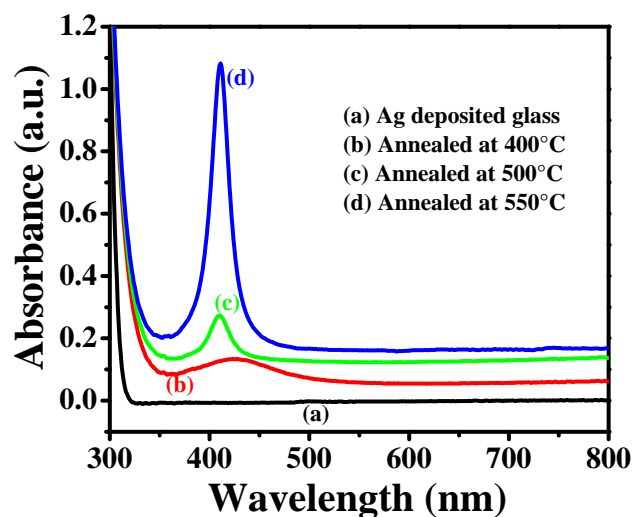


Fig. 1. Absorption spectra of silver deposited glass samples (a) before and after annealed at (b) 400°C, (c) 500°C, (d) 550°C temperature.

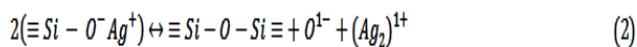
Assuming the free particle behavior of electrons the size of silver nanoparticles was calculated using the formula given by Eq. (1) [17, 18].

$$d = \frac{h v_f}{\pi \Delta E_{1/2}} \quad (1)$$

where, d is the diameter of the nanoparticles, v_f (1.39×10^6 m/sec) is the Fermi velocity of electrons in bulk silver, h is the Planck's constant and $\Delta E_{1/2}$ is the FWHM of the absorption band. The above equation is valid as long as the dimension of silver nanoparticles is smaller than the mean free path of the electrons in the bulk metal [1, 19]. The mean free path of electrons is about 27 nm at room temperature for bulk silver [20]. Using the above formula, the size of silver nanoparticles at an annealing temperature of 400°C has been calculated to be around 4.6 nm. A further increase in annealing temperature to 500°C, leads to a further narrowing of the SPR peak and the size of silver nanoparticles is estimated to be 8.9 nm. At an annealing

temperature of 550°C, size of silver nanoparticles comes out to be 10.0 nm. This result shows that the size of silver nanoparticles increases with increasing annealing temperature. This may be attributed to the diffusion-limited aggregation of silver nanoparticles.

When the Ag-deposited glasses are subjected to thermal annealing, due to annealing SiO_2 network of glass is ruptured and silver atoms diffuse into the glassy matrix. Silver so introduced into glass is mostly embraced of Ag^+ with a minor population of Ag^0 atoms. The Ag^0 atoms have an absorption wavelength of approximately 200 nm i.e. they do not have absorption in visible region. At low annealing temperature no silver nanoparticle formation occurs or size of silver nanoparticles is less than 1nm. However as the annealing temperature increases silver ions (Ag^+) are further reduced to silver atoms (Ag^0), which then in turn form silver nanoparticles with larger sizes. The electrons required for silver reduction are extracted from atoms that are intrinsic to the glass, namely nonbridging oxygen (NBO) atoms by the following equations [21]



As annealing temperature increases further, the following reduction reaction may take place resulting in an increased amount of silver in our sample (intense coloration and strong SPR band).



Silver-glass nanocomposite samples were further characterized using FE-SEM alongwith EDAX. **Fig. 2** depicts the morphology and distribution of Ag-glass nanocomposite samples annealed at 550°C obtained using FE-SEM and EDAX. This EDAX spectrum shows a peak at 3 keV that confirms the presence of silver within the host matrix. The rest of the lines of the EDAX spectrum correspond to other elements such as Si, Ca, and Na etc. present in the glass matrix.

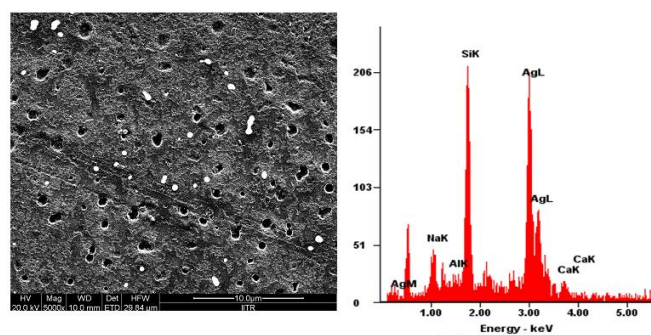


Fig. 2. FE-SEM image of silver deposited samples annealed at 550°C.

The presence of Ag nanoparticles in glass was further confirmed using TEM measurements. **Fig. 3** shows the TEM micrograph of silver deposited glass sample annealed at 550°C and size distribution of Ag nanoparticles as obtained from TEM image. TEM investigations reveal that Ag nanoparticles were well dispersed inside a glass matrix

with an average diameter of 8 ± 2 nm. The size calculated using TEM agrees fairly well with the size determined using the UV-Visible absorption spectra of the corresponding sample.

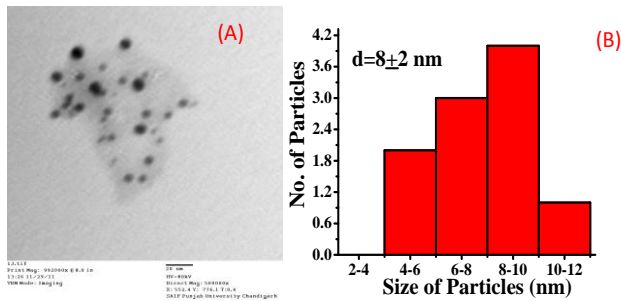


Fig. 3. (A) TEM micrograph showing the silver nanoparticles in the glass sample annealed at 550°C. (B) Size distribution of Ag nanoparticles.

Fig. 4 shows the transmittance (%T) and reflectance (%R) spectra of glass and Ag-glass nanocomposite samples as a function of wavelength in the range 300-800 nm. All samples show a dip in optical transmittance spectra corresponding to the surface plasmon resonance energy of Ag nanoparticles embedded in soda glass. It is clear from **Fig. 4** the transmission and reflection coefficient decreases nearly at wavelength 427 nm while the absorbance coefficient, on the contrary, increases. This sharp fall in transmittance can be of potential use in large area selective optical filters.

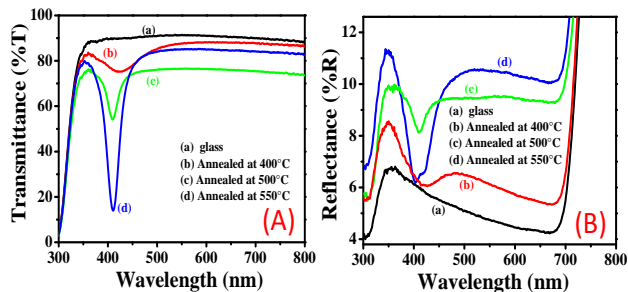


Fig. 4. (A) Transmission spectra of glass and Ag-glass nanocomposite samples. (B) Reflection spectra of glass and Ag-glass nanocomposite samples.

The complex refractive index and dielectric function characterize the optical properties of any solid materials. Refractive Index dispersion plays an important role in the research for optical materials, because it is a significant factor in optical communication and in designing devices for spectral dispersion. Refractive index of the prepared Ag-glass nanocomposite samples was determined from transmittance and reflectance spectra. In the case of normal light incidence, the reflectivity, R , may be expressed in terms of the real refractive index, n , and extinction coefficient, k , by the following Eqs. [22-24].

$$T(\lambda) = (1 - R) \exp\left(\frac{-4\pi kx}{\lambda}\right) \quad (5)$$

$$R = \frac{(n-1)^2 + k^2}{(n+1)^2 + k^2} \quad (6)$$

Solving Equation (6) for refractive index (n) the relation becomes:

$$n = \frac{(1+R) + \sqrt{4R - (1-R)^2 k^2}}{(1-R)} \quad (7)$$

where, k is the extinction coefficient given by:

$$k = \frac{\alpha \lambda}{4\pi} \quad (8)$$

where, α is the optical density and λ is the wavelength of the light used. **Fig. 5** shows the variation of the refractive index and extinction coefficient of resulting Ag-glass nanocomposite films with wavelength. The evaluation of refractive indices of optical materials is of considerable importance for applications in integrated optical devices such as switches, filters and modulators, etc., where the refractive index of a material is the key parameter in the design of a device.

It can be discerned from **Fig. 5** that the refractive index that was measured at visible wavelengths became more pronounced for silver nanoparticles embedded glass samples as compared to glass. However due to incorporation of silver nanoparticles of size 8 ± 2 nm in glass there is a significant increase in the value of refractive index from 1.52 (glass) to 1.96 (Ag-glass nanocomposite formed at an annealing temperature of 550°C). The large value of n and k indicate that the resulting Ag-glass nanocomposite is absorbing the light [25, 26].

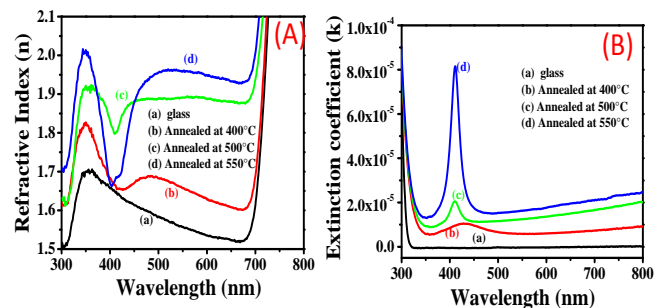


Fig. 5. (A) Variation of refractive index (n) with wavelength for glass and Ag-glass nanocomposite. (B) Variation of extinction coefficient (k) with wavelength for glass and Ag-glass nanocomposite.

It is well known that polarizability of any solid is proportional to its dielectric constant. The real (ϵ_1) and imaginary (ϵ_2) parts of the complex dielectric constant are expressed as-

$$\epsilon_1 = n^2 - k^2 \quad (9)$$

$$\epsilon_2 = 2nk \quad (10)$$

The variation of real and imaginary parts of the dielectric constant with wavelength calculated using Eqs. (9) and (10) of glass and Ag-glass nanocomposite samples are shown in **Fig. 6**. A significant increase in the value of

real part of dielectric constant from 2.4 for glass to 3.8 for Ag-glass nanocomposite formed after annealing at 550°C was observed. Thus with the insertion of silver nanoparticles of size 8 ± 2 nm in glass the dielectric constant of resulting nanocomposite increases drastically.

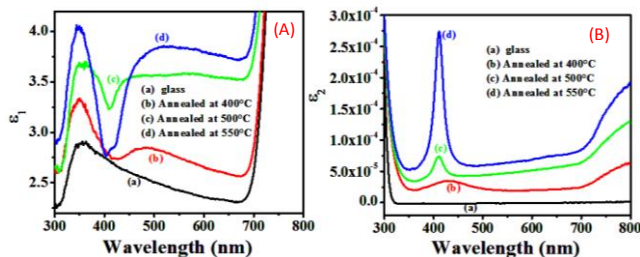


Fig. 6. (A) Variation of real part of dielectric constant with wavelength for glass and Ag-glass nanocomposite samples. (B) Variation of imaginary part of dielectric constant with wavelength for glass and Ag-glass nanocomposite samples.

In the normal dispersion region (transparent region), the refractive index dispersion has been analyzed using the single oscillator model developed by Wemple and DiDomenico [27-29]. They introduced an energy parameter E_d , which is a measure of the strength of interband optical transition to describe the dispersion of the refractive index. In terms of this dispersion energy E_d and single oscillator energy E_o ; the refractive index (n) at frequency (ν) can be written as [30]:

$$n^2 - 1 = \frac{E_d E_o}{[E_o^2 - (h\nu)^2]} \quad (11)$$

where, h is the Planck's constant, ν is the frequency, $h\nu$ is the photon energy, E_o is the single-oscillator energy and E_d is the dispersion energy, which is a measure of the strength of interband optical transitions. The dispersion parameters E_o and E_d can be obtained according to Eq. (11) by a simple plot of $(n^2 - 1)^{-1}$ versus $(h\nu)^2$ as shown in Fig. 7. The values of E_o and E_d can be directly determined from the slope $(E_d E_o)^{-1}$ and the intercept (E_o/E_d) on the vertical axis. The obtained values of the dispersion parameters E_o and E_d are listed in Table 1. The oscillator energy gap E_o can be considered as an average optical band gap [31].

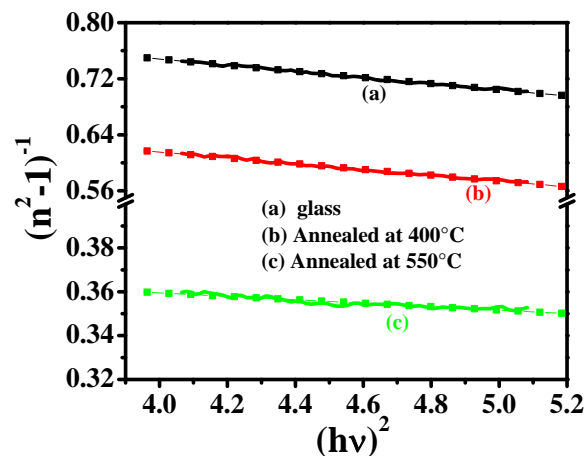


Fig. 7. Plots of $(n^2 - 1)^{-1}$ versus $(h\nu)^2$ for glass and Ag-glass nanocomposite samples.

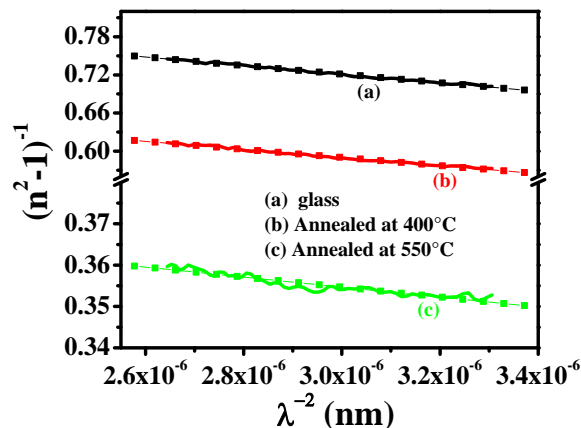


Fig. 8. Plots of $(n^2 - 1)^{-1}$ versus λ^{-2} for glass and Ag-glass nanocomposite samples.

From the dependence of the refractive index on the wavelength, the long wavelength refractive index (n_∞), average interband oscillator wavelength (λ_o) and the average oscillator strength (S_o) were obtained for the present system using the single term Sellmeir oscillator [32] as follows:

$$n^2 - 1 = \frac{S_o \lambda_o^2}{\left(1 - \frac{\lambda^2}{\lambda_o^2}\right)} \quad (12)$$

where, λ is the wavelength of incident light, λ_o is the average oscillator position and $S_o = n_\infty^2 - 1/\lambda_o^2$ is the average oscillator strength. The parameters S_o and λ_o in Eq. (12) can be obtained experimentally by plotting $(n^2 - 1)^{-1}$ versus λ^{-2} as shown in Fig. 8. The slope of the resulting straight line gives $1/S_o$ and the infinite-wavelength intercept gives $1/S_o \lambda_o^2$. The dependence of n_∞ , λ_o and S_o on different annealing temperature can be seen in Table 1. Drastic changes in dispersion parameters of resulting nanocomposite were observed. These parameters increase significantly for glass annealed at 550°C while below this temperature not much change was observed. The values obtained by this method are suitable for many scientific studies and technological applications, such as gas sensors, heat mirrors, transparent electrodes, solar cells and piezoelectric devices.

Table 1. Values of optical parameters for silver-glass nanocomposites.

Annealing Temp (°C)	E_d (eV)	E_o (eV)	n_∞	λ_o (nm)	$S_o \times 10^{13} (\text{m}^{-2})$
Virgin glass	4.96	4.46	1.45	273.72	1.48
400	5.56	4.48	1.51	285.58	1.57
550	18.05	7.22	1.88	175.69	8.28

Fig. 9 shows the photoluminescence spectra of glass and silver-glass nanocomposite samples annealed at different temperatures. At the excitation wavelength of 270 nm, silver deposited samples annealed at 300°C and 400°C show a broad emission band at 365 and 367 nm

respectively. Samples annealed at 500°C show two intense broad emission bands centred at around 382 nm and 435 nm. When the annealing temperature is further increased to 550°C the two bands are shifted to 372 and 442 nm respectively, however these bands are less intense than the bands observed in the samples annealed at 500°C. It is widely quoted that the incorporation of silver ions in crystals and glassy matrices causes the activation of a characteristic PL response, owing to electronic transitions between the $4d^{10}$ ground state and levels of the $4d^95s^1 Ag^+$ configuration [33-35]. These transitions are parity forbidden in free ion, where as they are partially allowed in a solid (crystalline or glassy matrix) by electronic coupling with lattice vibrations of odd-parity. The ground state of free silver ion is 1S_0 and the excited state of free silver ion is split into number of energy states 3D_3 , 3D_2 , 3D_1 and 1D_2 (Russell-Saunders states arising from $4d^95s^1 Ag^+$ configuration) in increasing order of energy. Transitions from 3D_j (where $j = 3, 2, 1$) state to ground state leads to lower energy (higher wavelength) emission whereas transitions from 1D_2 to ground state results in higher energy (lower wavelength) emission [36]. Thus it is reasonable to ascribe the emission band displayed at lower wavelength to spin allowed transitions from the 1D_2 state to the ground 1S_0 state and the emission bands appearing at higher wavelength can be assigned to spin-forbidden transitions from 3D_j states to 1S_0 states. Furthermore, PL intensity is maximum at the annealing temperature of 500°C, but when temperature is increased further to 550°C PL intensity decreases. It is well known that Ag^+ ions are luminescent in nature in both crystalline and glassy matrices [37]. In contrast, no PL emission due to Ag^0 atoms has been reported to the best of our knowledge. In view of this, we can say that increase in PL intensity at an annealing temperature of 500°C could be due to the increase of volume fraction of Ag^+ in the bulk of the glass matrix and the drastic decrease in PL intensity with further increase in annealing temperature can be due to the conversion of Ag^+ to Ag^0 . Hence increase in annealing temperature from 500°C to 550°C leads to the swift growth of silver nanoparticles and that might have resulted in the diminishing of PL intensity.

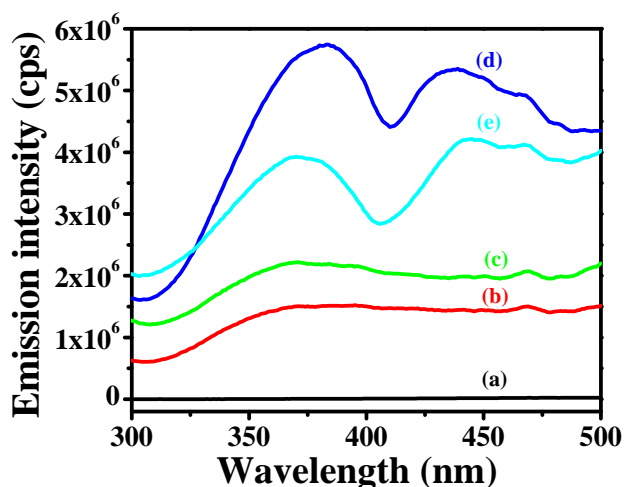


Fig. 9. Photoluminescence spectra of (a) glass, Ag deposited glass samples annealed at temperatures (b) 300°C, (c) 400°C, (d) 500°C, (e) 550°C excited at an excitation wavelength of 270 nm.

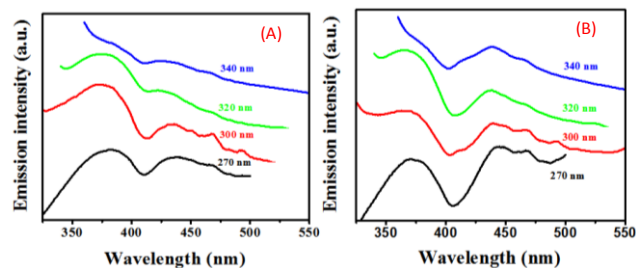


Fig. 10. (A) Photoluminescence emission spectra for Ag deposited glass sample annealed at 500°C at different excitation wavelengths. (B) Photoluminescence emission spectra for Ag deposited glass sample annealed at 550°C at different excitation wavelengths.

The excitation wavelength plays an important role in the PL spectra from silver nanoparticles. Hence effect of different excitation wavelengths on, PL spectra of Ag deposited glass samples annealed at 500°C and 550°C have been studied extensively. Fig. 10(A) and (B) shows emission spectra obtained for silver deposited glass samples annealed at 500°C and 550°C respectively, excited at wavelengths in the range of 270-340 nm. From Fig. 10(A) and (B) it is clear that by increasing the excitation wavelength from 270 to 340 nm, a blueshift in emission peak occurs for band appearing at higher wavelength i.e the band appearing due to spin-forbidden transitions from 3D_j states to 1S_0 states. This shift in band emission to shorter wavelengths with increasing excitation wavelength may be due to the overlapping of different emission centers due to the presence of Ag^+-Ag^0 pairs. Also from these figures it is clear that as the excitation wavelength is increasing, the peak on higher wavelength side is evolving while peak at lower wavelength is diminishing. This typical behaviour of band emission can be explained by two mechanisms: a more effective internal relaxation from the photo-excited states to the lower emitting states, and /or energy transfer between the ions close to each other [38]. The emission spectrum also shows a slight dip (~ 410 nm) which can be attributed to surface plasmon absorption of Ag nanoparticles.

Conclusion

In summary, we can conclude that thermal evaporation followed by thermal annealing is an effective method to synthesize Ag-glass nanocomposite. After annealing, these particles were reduced to Ag^0 and subsequently form silver nanoparticles even in oxidizing atmosphere like air. The UV-Visible spectrum confirmed the formation of Ag nanoparticles in glass with a surface plasmon band at 427 nm. From the absorption spectra the size of the Ag nanoparticles in glass was found to be 10 nm (at 550°C) agrees well with transmission electron microscopy. The optical constants such as refractive index (n), extinction coefficient (k) and real (ϵ_1) and imaginary (ϵ_2) parts of dielectric constant were found to increase significantly for resulting Ag-glass nanocomposite samples. The refractive index (n) values of the resulting nanocomposite increases from 1.52 to 1.96 and dielectric constant increases from 2.4 to 3.8 with incorporation of Ag nanoparticles of size 10 nm in glass matrix. The optical dispersion parameters E_0 and E_d using Wemple and DiDomenico model were also analyzed and it was established that the values of these parameters

increases with increasing the annealing temperature. Photoluminescence spectra of silver glass nanocomposite samples are due to the presence of Ag⁺ ion.

Reference

- Keirbeg, U.; Vollmer, M. *Optical Properties of Metal Cluster*, Springer, New York, **1995**.
- Tiwari, A.; Mishra, A. K.; Kobayashi, H.; Turner, A. P. F. *Intelligent Nanomaterials*, Wiley-Scrivener Publishing LLC, USA, ISBN 978-04-709387-99, **2012**.
DOI: [10.1002/9781118311974](https://doi.org/10.1002/9781118311974)
- Singh, R. P.; Tiwari, A.; Pandey, A. C. *J. Inorg. Organomet. Polym.* **2011**, *21*, 788.
DOI: [10.1007/s10904-011-9554-ys](https://doi.org/10.1007/s10904-011-9554-ys)
- Akman, E.; Genc Oztoprak, B.; Gunes, M.; Kacar, E.; Demir, A. *Photon. Nano. Fund. Appl.* **2011**, *9*, 276.
DOI: [10.1016/j.photonics.2011.05.004](https://doi.org/10.1016/j.photonics.2011.05.004)
- Stalmashonak, A.; Abdolvand, A.; Seifert, G. H. *Appl. Phys. Lett.* **2011**, *99*, 201904.
DOI: [10.1063/1.3660740](https://doi.org/10.1063/1.3660740)
- Hallermann, F.; Rockstuhl, C.; Fahr, S.; Seifert, G.; Wackerow, S.; Graener, H.; Plessen, G. v.; Lederer, F. *phys. stat. sol.* **2008**, *205*, 2844.
DOI: [10.1002/pssa.200880451](https://doi.org/10.1002/pssa.200880451)
- Stalmashonak, A.; Seifert, G.; Unal, A. A.; Skrzypczak, U.; Podlipensky, A.; Abdolvand, A.; Graener, H. *Appl. Opt.* **2009**, *48*, F37.
DOI: [10.1364/AO.48.000F37](https://doi.org/10.1364/AO.48.000F37)
- Fleming, L. A. H.; Wackerow, S.; Hourd, A. C.; Gillespie, W. A.; Seifert, G.; Abdolvand, A. *Opt. Express* **2012**, *20*, 22579.
DOI: [10.1364/OE.20.022579](https://doi.org/10.1364/OE.20.022579)
- Niry, M. D.; Mostafavi-Amjad, J.; Kholesifard, H. R.; Ahangary, A.; Azizian-Kalandaragh, Y. *J. Appl. Phys.* **2012**, *111*, 033111.
DOI: [10.1063/1.3684552](https://doi.org/10.1063/1.3684552)
- Bahniwal, S.; Sharma, A.; Aggarwal, S.; Deshpande, S. K. *J. Appl. Phys.* **2008**, *104*, 064318.
DOI: [10.1063/1.2982373](https://doi.org/10.1063/1.2982373)
- Liu, Z.; Wang, H.; Li, H.; Wong, X. *Appl. Phys. Lett.* **1998**, *72*, 1823.
DOI: [10.1063/1.121196](https://doi.org/10.1063/1.121196)
- Gangopadhyay, P.; Kesavamoorthy, R.; Nair, K. G. M.; Dhandapani, R. *J. Appl. Phys.* **2000**, *88*, 4975.
DOI: [10.1063/1.1290739](https://doi.org/10.1063/1.1290739)
- Takele, H.; Greve, H.; Pochstein, C.; Zaporozhtchenko, V.; Faupel, F. *Nanotechnology* **2006**, *17*, 3499.
DOI: [10.1088/0957-4484/17/14/023](https://doi.org/10.1088/0957-4484/17/14/023)
- Hsieh, J. H.; Li, Chuan; Wu, Y. Y.; Jang, S. C. *Thin Solid Films* **2011**, *519*, 7124.
DOI: [10.1016/j.tsf.2011.04.087](https://doi.org/10.1016/j.tsf.2011.04.087)
- Gangopadhyay, P.; Kesavamoorthy, R.; Bera, S.; Magudapathy, P.; Panigrahi, B. K.; Narasimhan, S. V. *Phys. Rev. Lett.* **2005**, *94*, 047403.
DOI: [10.1103/PhysRevLett.94.047403](https://doi.org/10.1103/PhysRevLett.94.047403)
- Garcia, M. A.; Garcia-Heras, M.; Cano, E.; Bastidas, J. M.; Villegas, M. A.; Montero, E.; Llopis, J.; Sada, C.; De Marchi, G.; Battaglin, G.; Mazzoldi, P. *J. Appl. Phys.* **2004**, *96*, 3737.
DOI: [10.1063/1.1778473](https://doi.org/10.1063/1.1778473)
- Arnold, G. W. *J. Appl. Phys.* **1975**, *46*, 4466.
DOI: [10.1063/1.321422](https://doi.org/10.1063/1.321422)
- Rozra, J.; Saini, I.; Sharma, A.; Chandak, N.; Aggarwal, S.; Dhiman, R.; Sharma, P. K. *Mater. Chem. Phys.* **2012**, *134*, 1121.
DOI: [10.1016/j.matchemphys.2012.04.004](https://doi.org/10.1016/j.matchemphys.2012.04.004)
- Karthikeyan, B. *J. Appl. Phys.* **2008**, *103*, 114313.
DOI: [10.1063/1.2936879](https://doi.org/10.1063/1.2936879)
- Kittel, C. *Introduction to Solid State Physics*, 8th ed., Wiley Eastern, India, **2007**.
- Wackerow, S.; Seifert, G.; Abdolvand, A. *Opt. Mater. Express* **2011**, *1*, 1224.
DOI: [10.1364/OME.1.001224](https://doi.org/10.1364/OME.1.001224)
- Sole, J. G.; Bausa, L. E.; Jaque, D. *An Introduction to the Optical Spectroscopy of Inorganic Solids*, John Wiley & Sons, England, **2005**.
- Fink, D. *Fundamentals of Ion-Irradiated Polymers*, Springer-Verlag, Berlin, **2004**.
- Al-Agel, F. A. *Vacuum* **2011**, *85*, 892.
DOI: [10.1016/j.vacuum.2011.01.006](https://doi.org/10.1016/j.vacuum.2011.01.006)
- Ilyas, M.; Zulfeqar, M.; Zishan, H.; Husain, M. *Opt. Mater.* **1998**, *11*, 67.
DOI: [10.1016/S0925-3467\(98\)00016-0](https://doi.org/10.1016/S0925-3467(98)00016-0)
- Caglara, M.; Ilican, S.; Caglar, Y.; Sahin, Y.; Yakuphanoglu, F.; Hur, D. *Spectrochimica Acta Part A* **2008**, *71*, 621.
DOI: [10.1016/j.saa.2008.01.022](https://doi.org/10.1016/j.saa.2008.01.022)
- DiDomenico, M.; Wemple, S. H. *J. Appl. Phys.* **1969**, *40*, 720.
DOI: [10.1063/1.1657458](https://doi.org/10.1063/1.1657458)
- Ammar, A. H. *Appl. Surf. Sci.* **2002**, *201*, 9.
DOI: [10.1016/S0169-4332\(02\)00223-4](https://doi.org/10.1016/S0169-4332(02)00223-4)
- Yakuphanoglu, F.; Sekerci, M. *J. Mol. Struct.* **2005**, *751*, 200.
DOI: [10.1016/j.molstruc.2005.05.021](https://doi.org/10.1016/j.molstruc.2005.05.021)
- Gasanly, N. M. *Mater. Chem. Phys.* **2012**, *136*, 259.
DOI: [10.1016/j.matchemphys.2012.06.064](https://doi.org/10.1016/j.matchemphys.2012.06.064)
- Wemple, S. H.; DiDomenico, Jr. M. *Phys. Rev. B* **1971**, *3*, 1338.
DOI: [10.1103/PhysRevB.3.1338](https://doi.org/10.1103/PhysRevB.3.1338)
- Zidan, H. M.; El-khodary, A.; El-Sayed, I. A.; El-bohy, H. I. *J. Appl. Polym. Sci.* **2010**, *117*, 1416.
DOI: [10.1002/app.31939](https://doi.org/10.1002/app.31939)
- Paje, S. E.; Llopis, J.; Villegas, M. A.; Garcia, M. A.; Fernandez Navarro, J. M. *Appl. Phys. A* **1998**, *67*, 429.
DOI: [10.1007/s003390050799](https://doi.org/10.1007/s003390050799)
- Borsella, E.; Battaglin, G.; Garcia, M. A.; Gonella, F.; Mazzoldi, P.; Polloni, R.; Quaranta, A. *Appl. Phys. A* **2000**, *71*, 125.
DOI: [10.1007/s003390000472](https://doi.org/10.1007/s003390000472)
- Pal, S.; De, G. *Mater. Res. Bull.* **2009**, *44*, 355.
DOI: [10.1016/j.materresbull.2008.05.011](https://doi.org/10.1016/j.materresbull.2008.05.011)
- Jimenez, J. A.; Lysenko, S.; Liu, H. *J. Appl. Phys.* **2008**, *104*, 054313.
DOI: [10.1063/1.2976171](https://doi.org/10.1063/1.2976171)
- Villegas, M. A.; Garcia, M. A.; Llopis, J.; Fernandez Navarro, J. M. *J. Sol-Gel Sci. Technol.* **1998**, *11*, 251.
DOI: [10.1023/A:1008654228678](https://doi.org/10.1023/A:1008654228678)
- Meijerink, A.; van Heek, M. M. E.; Blasse, G. *J. Phys. Chem. Solids* **1993**, *54*, 901.
DOI: [10.1016/0022-3697\(93\)90216-E](https://doi.org/10.1016/0022-3697(93)90216-E)

Advanced Materials Letters

Publish your article in this journal

ADVANCED MATERIALS Letters is an international journal published quarterly. The journal is intended to provide top-quality peer-reviewed research papers in the fascinating field of materials science particularly in the area of structure, synthesis and processing, characterization, advanced-state properties, and applications of materials. All articles are indexed on various databases including DOAJ and are available for download for free. The manuscript management system is completely electronic and has fast and fair peer-review process. The journal includes review articles, research articles, notes, letter to editor and short communications.

